

RESEARCH OUTPUTS / RÉSULTATS DE RECHERCHE

Coupled cluster investigation of the vibrational and electronic second and third harmonic scattering hyperpolarizabilities of the water molecule

Beaujean, Pierre; Champagne, Benoît

Published in:

The journal of chemical physics

DOI:

[10.1063/1.5110375](https://doi.org/10.1063/1.5110375)

Publication date:

2019

Document Version

Early version, also known as pre-print

[Link to publication](#)

Citation for pulished version (HARVARD):

Beaujean, P & Champagne, B 2019, 'Coupled cluster investigation of the vibrational and electronic second and third harmonic scattering hyperpolarizabilities of the water molecule', *The journal of chemical physics*, vol. 151, no. 6, 064303. <https://doi.org/10.1063/1.5110375>

General rights

Copyright and moral rights for the publications made accessible in the public portal are retained by the authors and/or other copyright owners and it is a condition of accessing publications that users recognise and abide by the legal requirements associated with these rights.

- Users may download and print one copy of any publication from the public portal for the purpose of private study or research.
- You may not further distribute the material or use it for any profit-making activity or commercial gain
- You may freely distribute the URL identifying the publication in the public portal ?

Take down policy

If you believe that this document breaches copyright please contact us providing details, and we will remove access to the work immediately and investigate your claim.

Coupled Cluster investigation of the vibrational and electronic second and third harmonic scattering hyperpolarizabilities of the water molecule

Pierre Beaujean¹ and Benoît Champagne^{1, a)}

Laboratory of Theoretical Chemistry, Unit of Theoretical and Structural Physical Chemistry, Namur Institute of Structured Matter, University of Namur, Rue de Bruxelles 61, B-5000 Namur, Belgium

(Dated: 21 June 2019)

The vibrational contributions to the average polarizability ($\bar{\alpha}$), to the second harmonic scattering (SHS) first hyperpolarizability (β_{SHS}) and depolarization ratio (DR_{SHS}), as well as to the third harmonic scattering (THS) second hyperpolarizability (γ_{THS}) and depolarization ratio (DR_{THS}) have been evaluated for the water molecule using the Bishop and Kirtman perturbative theory approach, in combination with finite differentiation techniques to evaluate the higher-order derivatives. From a hierarchy of Coupled Clusters techniques and extended atomic basis sets, the CCSD/d-aug-cc-pVTZ level has been selected to assess the importance of the ZPVA contributions and of the pure vibrational contributions with respect to their electronic counterparts. This is the first investigation demonstrating electronic and vibrational SHS and THS responses can be computed for small molecules, with the perspective of performing comparisons with recent experimental data [Anal. Chem. **89**, 2964 (2017) and J. Phys. Chem. C **121**, 8510 (2017)]. Numerical results on the water molecule highlight that i) the vibrational contributions to the dynamic $\bar{\alpha}$, β_{SHS} , and γ_{THS} are small but non negligible, ii) they amount to respectively 3, 10, and 4% at the typical 1064 nm wavelength, iii) the mechanical anharmonicity term dominates the zero-point vibrational average contribution, iv) the double harmonic terms dominate the pure vibrational contributions, v) the stretching vibrations provide the largest contributions to the dynamic (hyper)polarizabilities, and vi) these conclusions are strongly impacted in the static limit where the vibrational contributions are much larger, in particular the double harmonic pure vibrational terms, and even more in the case of the first hyperpolarizability.

Keywords: first and second hyperpolarizabilities, Coupled Cluster methods, electronic versus vibrational contributions, second and third harmonic scattering

^{a)}Electronic mail: benoit.champagne@unamur.be

I. INTRODUCTION

The interactions between light and matter constitute a bottomless topic, with scientific, technological, philosophical, and medical aspects. Among these, nonlinear effects present their own interest and characteristics. Since their first observations, usually attributed to the discovery of lasers, many nonlinear optical (NLO) effects have been revealed and their study has led to the development of analytical or spectroscopic tools for characterizing molecular structures and for imaging as well as to the elaboration of optics-based devices.¹⁻⁴ The present work focuses on the Second Harmonic Scattering^{4,5} (SHS, also called hyper-Rayleigh Scattering, HRS) and Third Harmonic Scattering (THS)^{6,7} phenomena. At the molecular scale, the NLO effects, including SHS and THS, are described by the first (β) and second (γ) hyperpolarizabilities and numerous studies have dwelled on their relationships with the molecular structure.⁸⁻¹³ In parallel to instrumental developments as well as to synthesis and characterization of highly active compounds, the hyperpolarizabilities have been a topic of intense theoretical and computational activities to derive structure-property relationships in order to design compounds with high efficiency but also because the hyperpolarizabilities are challenging quantities to calculate and to interpret.^{10,14} In particular, numerous works have highlighted the large electron correlation effects,¹⁵⁻¹⁹ the impact of the surrounding (solvent, self-assembled monolayer, solid),²⁰⁻²⁵ the specific frequency dispersion,^{26,27} and the importance of the vibrational contributions. This last topic has been the subject of extended studies, to select reliable computational levels of approximation²⁸⁻³⁴ as well as to unravel the structure-property relationships for molecules,³⁵⁻³⁸ clusters,^{39,40} solids⁴¹, or new materials.⁴²⁻⁴⁴ Owing its small size and omnipresence, the determination of the water electrical properties has always been the subject of numerous investigations and it was often considered when testing new methods, for instance in the case of the polarizability,⁴⁵ the first and second hyperpolarizabilities,⁴⁶ and their related multipolar properties.^{47,48}

When electron correlation is included at an appropriate level and with a well-chosen basis set, usually an extended basis set with diffuse functions, accurate electronic (hyper)polarizability values are obtained.⁴⁹⁻⁵⁴ Nevertheless, within the Born-Oppenheimer approximation, along with this electronic contribution, they are additional contributions, called vibrational contributions. They originate from the electric field-induced nuclear reorganizations as well as from the electric field dependence of the potential energy surface.⁵⁵ Within

the perturbation theory approach, these vibrational responses are divided into pure vibrational and zero-point vibrational average (ZPVA) contributions. Their expressions have been derived by Bishop, Luis, and Kirtman^{56–58} by expanding in Taylor series the potential energy surface and the electrical properties around the equilibrium geometry, leading to contributions of higher and higher orders in mechanical and electrical anharmonicities.

Previous studies^{59–68} have shown that, in the static limit as well as for specific NLO processes involving one or more static field, the correction that originates from the pure vibrational contributions can be of similar magnitude to the electronic contribution and cannot be neglected. On the other hand, in the case of “fully” optical phenomena, like SHS and THS, those contributions are usually neglected. Indeed, the pure vibrational part is expected to be much smaller at optical frequencies because it is damped by the $(\omega_a/\omega)^{2n}$ ($n \geq 1$) multiplicative factor, where ω_a is a vibrational mode (angular) frequency and ω is the frequency of the incident light. In addition, the ZPVA represents usually only a few percents of the electronic response and it is, therefore, often neglected. Moreover, there are fewer results on the ZPVA contributions since it is anharmonic in nature and it requires computationally expensive calculations of, at least, the cubic force constants as well as of second-order derivatives of the electrical properties with respect to the normal mode coordinates. In this paper, we address this simplification by tackling the water molecule with a hierarchy of Coupled Cluster (CC) methods combined with extended basis sets. The importance of the different vibrational contributions is then assessed as a function of ω , while the validity of Kleinmann’s symmetry conditions is checked. Emphasis is also put on the contributions of the different vibrational normal modes, in relation to their symmetry representation.

This paper is divided in five sections. After a description, in Section II, of the vibrational contributions to α , β and γ , and the target quantities, Section III presents the computational details. Then, in Section IV, the main results are presented and analyzed. First the effects of the level of approximation and of the atomic basis set are assessed. Then, using a selected method, the relative amplitudes of the vibrational contributions are discussed at the light of their electronic counterpart and they are traced back to the contributions of the vibrational normal modes. Moreover, comparisons are made with previous calculations of both the electronic and vibrational (hyper)polarizabilities of water. Finally conclusions are drawn in Section V.

II. THEORETICAL ASPECTS

A. Electronic and vibrational hyperpolarizabilities

At the molecular scale, the frequency-dependent polarizability, first and second hyperpolarizabilities are the Taylor series expansion coefficients of the molecular induced dipole moment as a function of external electric fields, \vec{F} , applied along the i, j, \dots directions (note that lower-case letters stand for coordinates in the molecular frame) and oscillating at frequencies $\omega_1, \omega_2, \dots$:

$$\begin{aligned} \Delta\mu_i(\vec{F}) = & \sum_j^{x,y,z} \alpha_{ij}(-\omega_\sigma; \omega_1) F_j(\omega_1) + \frac{1}{2!} \sum_{jk}^{x,y,z} \beta_{ijk}(-\omega_\sigma; \omega_1, \omega_2) F_j(\omega_1) F_k(\omega_2) \\ & + \frac{1}{3!} \sum_{jkl}^{x,y,z} \gamma_{ijkl}(-\omega_\sigma; \omega_1, \omega_2, \omega_3) F_j(\omega_1) F_k(\omega_2) F_l(\omega_3) + \dots \end{aligned} \quad (1)$$

with $\omega_\sigma = \sum_i \omega_i$. α_{ij} is an element of the polarizability tensor, β_{ijk} and γ_{ijkl} are elements of the first and second hyperpolarizability tensors, respectively. Depending on the combination of static and dynamic electric fields, different NLO processes arise. The SHS and THS responses are noted $\beta(-2\omega; \omega, \omega)$ and $\gamma(-3\omega; \omega, \omega, \omega)$, respectively.

When electric fields interact with a molecule, different phenomena occur. Within the clamped-nucleus approximation,⁵⁵ the effects on the electronic and nuclear motions are considered sequentially, rather than simultaneously. First, the electronic distribution changes, giving rise to the electronic responses, P^e , with $P = \alpha, \beta$, or γ . This induces a modification of the ground state potential energy surface, therefore of the equilibrium geometry and of the vibrational zero-point energy, leading to the so-called nuclear relaxation and curvature contributions to the (hyper)polarizabilities, or, globally, the vibrational responses, P^v . Note that, under the application of external electric fields, the molecule can also rotate to align its (induced) dipole moment on the external field but this contribution is neglected for optical electric fields because the molecular response time is too slow with respect to the incident light frequency.

The total electrical property, P^{tot} , reads therefore $P^{tot} = P^e + P^v$. To provide tractable equations, Bishop and Kirtman⁵⁶ started from the sum-over-states (SOS) perturbation theory expressions of the (hyper)polarizabilities in the adiabatic approximation⁶⁹, and decomposed these into two terms, the electronic [$P^e(\text{SOS})$] and the pure vibrational [$P^{pv}(\text{SOS})$]

contributions. These expressions were then further simplified by invoking the clamped nucleus approximation, leading to SOS expressions where the electronic states are employed instead of vibronic states. As a result, the corresponding electronic contribution [$P^e(\text{CN})$] involves a zero-point vibrational averaging over the vibrational ground state wavefunction of the electronic ground state so that it can be written as the sum of the electronic contribution at the equilibrium ground state geometry (P^e) and a ZPVA correction (ΔP^{ZPVA}). These ZPVA contributions present therefore the same type of frequency dispersion as their electronic counterparts. For $P^{pv}(\text{CN})$, Bishop and Kirtman⁵⁶ assumed that, in non-resonant regimes, optical frequencies can be neglected in comparison to electronic transition frequencies. Note that this approximation holds in the static and infinite frequency limit, but some corrections would be needed for optical fields, as discussed by Kirtman and Luis.⁷⁰ Finally, the treatment of Ref.⁵⁶ leads to the decomposition of the pure vibrational contributions P^{pv} into square bracket quantities, involving lower-order electrical properties:

$$\alpha^{pv} = [\mu^2], \quad (2)$$

$$\beta^{pv} = [\mu\alpha] + [\mu^3], \quad (3)$$

$$\gamma^{pv} = [\alpha^2] + [\mu\beta] + [\mu^2\alpha] + [\mu^4]. \quad (4)$$

Then, for both P^{pv} and ΔP^{ZPVA} quantities, it is assumed that the power series expansions of the electrical properties around the equilibrium geometry and of the potential energy are convergent. This allows treating electrical (when second- and higher-order derivatives of the electrical properties are considered) and mechanical (when third- and higher-order derivatives of the potential energy are considered) anharmonicities by ordinary double perturbation theory and writing the different quantities as sums of harmonic and anharmonic terms. In the present investigation, the following terms are included:

$$\Delta P^{ZPVA} = [P]^I, \quad (5)$$

$$\alpha^{pv} = [\mu^2]^0 + [\mu^2]^{\text{II}}, \quad (6)$$

$$\beta^{pv} = [\mu\alpha]^0 + [\mu^3]^I + [\mu\alpha]^{\text{II}}, \quad (7)$$

$$\gamma^{pv} = [\alpha^2]^0 + [\mu\beta]^0 + [\mu^2\alpha]^I + [\alpha^2]^{\text{II}} + [\mu\beta]^{\text{II}} + [\mu^4]^{\text{II}}, \quad (8)$$

where $[X]^0 = [X]^{0,0}$, $[X]^I = [X]^{1,0} + [X]^{0,1}$, and $[X]^{\text{II}} = [X]^{1,1} + [X]^{2,0} + [X]^{0,2}$. The $[X]^{m,n}$ notation associates m with the order of electrical anharmonicity and n with the order of

mechanical anharmonicity. Still, the expressions for $[X]^{2,0}$ and $[X]^{0,2}$ were truncated so that they do not contain third-order derivatives of electrical properties nor quartic force constants, respectively. The detailed expressions for those contributions were derived by Bishop, Luis, and Kirtman^{56–58} and are used in the present work.

B. Hyperpolarizability tensor components and target quantities

All components of the electronic and vibrational (hyper)polarizability tensors were calculated in order to evaluate quantities that can be extracted from experiment. For the polarizability, these quantities are its isotropic average ($\bar{\alpha}$) and its anisotropy ($\Delta\alpha$), defined as

$$\bar{\alpha} = \frac{1}{3} \sum_i^{x,y,z} \alpha_{ii}, \quad (9)$$

$$\Delta\alpha = \left[\frac{1}{2} \sum_{i,j}^{x,y,z} 3\alpha_{ij}^2 - \alpha_{ii}\alpha_{jj} \right]^{1/2}. \quad (10)$$

The higher-order target quantities are the second harmonic scattering first hyperpolarizability (β_{SHS}) and the third harmonic scattering second hyperpolarizability (γ_{THS}) as well as their depolarization ratios (DR_{SHS} and DR_{THS}):

$$\beta_{SHS} = \sqrt{\langle\beta_{ZZZ}^2\rangle + \langle\beta_{ZXX}^2\rangle}, \quad (11)$$

$$DR_{SHS} = \frac{\langle\beta_{ZZZ}^2\rangle}{\langle\beta_{ZXX}^2\rangle}, \quad (12)$$

$$\gamma_{THS} = \sqrt{\langle\gamma_{ZZZZ}^2\rangle + \langle\gamma_{ZXXX}^2\rangle}, \quad (13)$$

$$DR_{THS} = \frac{\langle\gamma_{ZZZZ}^2\rangle}{\langle\gamma_{ZXXX}^2\rangle}. \quad (14)$$

β_{SHS} and γ_{THS} characterize the scattering intensities for non-polarized incident light and observation of plane-polarized scattered light made perpendicularly to the propagation plane. $\langle\beta_{ZZZ}^2\rangle$ ($\langle\gamma_{ZZZZ}^2\rangle$) and $\langle\beta_{ZXX}^2\rangle$ ($\langle\gamma_{ZXXX}^2\rangle$) are orientational averages of the β (γ) tensor components describing the SHS (THS) intensities when the incident light is vertically- or horizontally-polarized, respectively. Their detailed expressions can be found in Refs. 71–74. Still, owing to its symmetry (water belongs to the C_{2v} point group) and specific NLO processes, out of the 27 (β) or 81 (γ) tensor components, only a reduced number of components have to be calculated. So, the number of non-zero independent tensor components amounts

to 3 (xx, yy and zz) for the polarizability, to 5 [x(xz), y(yz), zxx, zyy, and zzz, parentheses indicate permutations that leave invariant the tensor component] for the first hyperpolarizability, and 9 [xxxx, x(xyy), x(xzz), y(xxy), yyy, y(yzz), z(xxz), z(yyz), and zzzz] for the second hyperpolarizability.⁷² In the static limit, Kleinman's conditions are fulfilled and any permutation of the tensor indices leave invariant the tensor components so that the number of non-zero independent tensor components is further reduced to 3 and 6 for the first and second hyperpolarizabilities, respectively.

Symmetry has also an impact on the number of derivatives to calculate, *i.e.* the derivatives of the molecular electrical properties with respect to the vibrational normal coordinates (Appendix A). Indeed, the water molecule possesses three vibrational normal modes: a bending (associated with Q_1 , of A_1 irreducible representation), a symmetric (Q_2 , A_1) and an anti-symmetric (Q_3 , B_2) stretching.

To assess the importance of the electronic and vibrational contributions on the total value of a given (hyper)polarizability, a missing-contribution analysis was used, with \mathcal{C}_A a measure, in percents, of the A contribution:

$$\mathcal{C}_A = 100 \times \left\{ 1 - \frac{P^{(-A)}}{P^{tot}} \right\}, \quad (15)$$

where $P^{(-A)}$ is the property for which the A contribution is missing. For any tensor component, the curly bracket is equivalent to $\frac{P^A}{P^{tot}}$. The impact of a vibrational mode on a given vibrational contribution to P^v was assessed in the same way, using the missing mode analysis:

$$\mathcal{C}_a = 100 \times \left\{ 1 - \frac{P^{v(-a)}}{P^v} \right\}, \quad (16)$$

where $P^{v(-a)}$ is the vibrational property computed by using all the normal modes but mode a . All α , β , and γ quantities are given within the T convention (Eq. 1) in a.u.:

- 1 a.u. of $\alpha = 1.648 \times 10^{-41} \text{ C}^2 \text{ m}^2 \text{ J}^{-1} = 0.14818 \text{ \AA}^3$;
- 1 a.u. of $\beta = 3.6212 \times 10^{-42} \text{ m}^4 \text{ V}^{-1} = 3.2064 \times 10^{-53} \text{ C}^3 \text{ m}^3 \text{ J}^{-2} = 8.639 \times 10^{-33} \text{ esu}$;
- 1 a.u. of $\gamma = 7.423 \times 10^{-54} \text{ m}^5 \text{ V}^{-2} = 6.2354 \times 10^{-65} \text{ C}^4 \text{ m}^4 \text{ J}^{-3} = 5.0367 \times 10^{-40} \text{ esu}$.

III. COMPUTATIONAL ASPECTS

The water molecule lies in the YZ plane with its C_2 axis coinciding with the Cartesian Z axis (the oxygen atom points in the direction of negative Z). Its geometry was optimized in gas phase at different levels of approximation (HF, CCS⁷⁵, CC2⁷⁵, CCSD⁷⁶) and with different basis sets ([d-]aug-cc-pVXZ⁷⁷, with X=D, T). The static and dynamic (at 1500, 1300, 1064 and 694.3 nm wavelengths) electronic properties (polarizability, SHS first hyperpolarizability, and THS second hyperpolarizability) were computed at the same levels of approximation for both equilibrium and distorted geometries, using the linear,⁷⁸ quadratic (QRF),^{79,80} and cubic (CRF)^{81,82} response function methods.

In order to calculate the geometrical derivatives of the electrical properties with respect to the atomic Cartesian coordinates, the central finite difference method was employed and combined with the Romberg (or Richardson) quadrature ($k_{max}=4$, distortion amplitude = $0.01 a_0$, common ratio = 2) to remove higher-order contaminations.⁸³⁻⁸⁶ These derivatives were finally projected over the normal coordinates in order to obtain the derivatives with respect to the vibrational normal mode coordinates. At the Hartree-Fock level, the Hessian required to compute the vibrational normal modes and frequencies was calculated analytically, using the coupled-perturbed Hartree-Fock scheme, but the cubic force constants numerically, as the first-order derivatives of the Hessian using the same method as described above for the geometrical derivatives of the electrical properties. At the CC levels, both quadratic and cubic force constants were calculated from the analytical gradients, as their first- and second-order derivatives, respectively. The masses used for the hydrogen and oxygen atoms in the computation of the mass-weighted Hessian are $m_H=1.00794$ a.m.u. and $m_O=15.9994$ a.m.u.⁸⁷

The geometry optimizations and electrical property calculations were performed using Dalton 2016⁸⁸ while a homemade program was employed to calculate the numerical derivatives and the subsequent vibrational (hyper)polarizabilities. The SCF convergence was set to 10^{-11} a.u. and CPHF (or its CC counterparts) QRF and CRF convergences to 10^{-10} a.u.

IV. RESULTS AND DISCUSSIONS

A. Geometries and vibrational frequencies

Table S1 describes the impact of the level of approximation and basis set on the equilibrium geometrical parameters of the water molecule, which are also plotted in Fig. 1. Changes from double- to triple- ζ basis sets or from CCS to CCSD leads to concerted variations in the bond length and valence angle: when R increases, δ decreases. Going from double- to triple- ζ basis sets increases the valence angle by $0.3\text{-}0.4^\circ$ while a decrease of the bond length by $0.007\text{-}0.008\text{\AA}$ is observed when going from the CCS to CCSD level. On the other hand, the addition of a second set of diffuse functions has a much smaller effect. Then, electron correlation leads to a lengthening of the O-H bond by about 0.02\AA and to a smaller valence angle by about 2° . The differences between CC2 and CCSD are smaller.

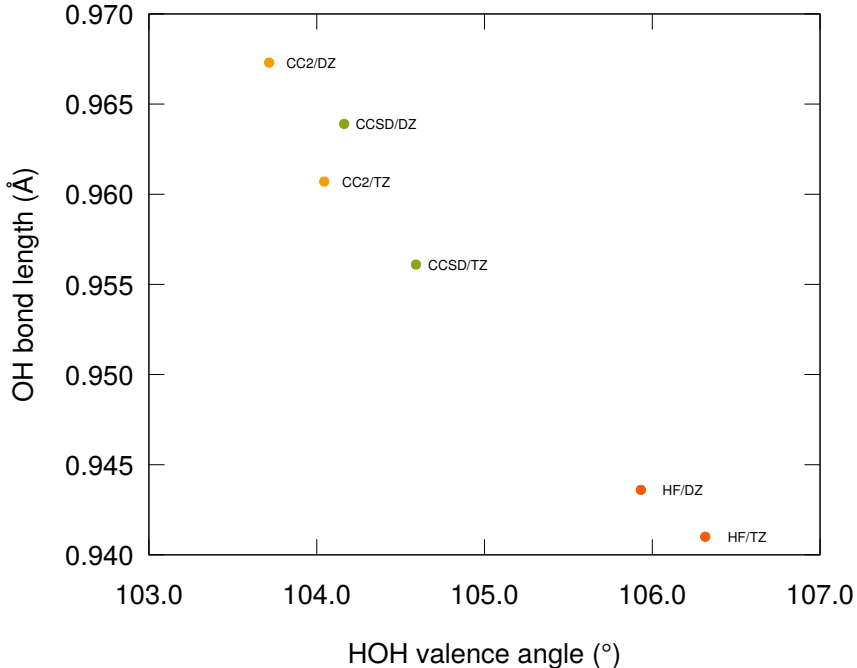


FIG. 1: Impact of the level of approximation and basis set (XZ=aug-cc-pVXZ) on the equilibrium geometrical parameters of water.

The impact of the method of calculation on the vibrational frequencies is presented in Table I. The effect of the basis set depends on the method and impacts mostly the stretching modes. While the HF frequencies vary by 5 to 15 cm^{-1} , there is a larger impact at the CC2

and CCSD levels (up to 50 cm^{-1} for the stretchings). On the other hand, the additional set of diffuse functions impacts the frequencies by less than 6 cm^{-1} , the B_2 stretching being mostly affected. Taking CCSD/d-aug-cc-pVTZ as reference, the HF frequencies evaluated with the same basis set are overestimated by 5% for the bending and by as much as 8% for the stretchings, while the CC2 frequencies are underestimated by less than 2%.

TABLE I: Basis set and electron correlation effects on the harmonic vibrational frequencies of water (ω_1 , A_1 bending; ω_2 , A_1 symmetric stretching; ω_3 , B_2 anti-symmetric stretching, in cm^{-1}).

	D			T		
	ω_1	ω_2	ω_3	ω_1	ω_2	ω_3
	aug-cc-pVXZ					
HF = CCS	1744.2	4130.0	4237.4	1745.0	4120.29	4222.6
CC2	1617.3	3770.6	3907.5	1619.0	3812.5	3935.0
CCSD	1649.8	3823.9	3939.4	1654.7	3880.8	3982.0
	d-aug-cc-pVXZ					
HF = CCS	1749.8	4130.1	4238.8	1745.8	4121.3	4222.5
CC2	1623.7	3768.6	3907.0	1620.9	3806.1	3929.0
CCSD	1656.3	3822.0	3938.9	1656.5	3874.3	3975.8

B. Polarizabilities and hyperpolarizabilities

The total (electronic + ZPVA + pv) static and dynamic (1064 nm) (hyper)polarizabilities calculated at the different levels of approximation are given in Tables II-IV. On the basis of our recent investigations on the first and second electronic hyperpolarizabilities of water, methanol, and dimethylether,^{54,74} the CCSD/d-aug-cc-pVTZ results are considered as reference values. This allows assessing, on the one hand, the contribution of electron correlation to the (hyper)polarizabilities, *i.e.* the differences between the HF and CCSD results, as well as to check how close or different are the more approximate CC2 values. On the other hand, these reference values are employed to estimate the importance of including a second set of diffuse functions and of using triple- ζ instead of double- ζ basis sets.

With respect to CCSD, the HF and CCS response property values are underestimated ($\Delta\alpha$ and DR_{THS} are overestimated), while CC2 overestimates the different quantities ($\Delta\alpha$ and DR_{THS} are underestimated). These results, on both the static and dynamic linear and nonlinear responses, are consistent with the results on the electronic responses only.^{54,74} Within the four basis sets employed in this work, basis set effects on the isotropic polarizability are of the order of 2%. They increase to about 10% for β_{SHS} . For γ_{THS} these can attain 50%. Still, like in Ref. 74, the basis set effects on the depolarization ratios are much larger. These are also stronger on the polarizability anisotropy than on the average polarizability.

The vibrational contribution to the average polarizability range between 5 and 7% in the static limit and decreases to about 3% at 1064 nm. Changing the basis set has a negligible influence on these percentages whereas changing the method leads to variations of the order of 1% with respect to the Hartree-Fock case. The impact of including the vibrational contributions to the polarizability anisotropy is much stronger, with contributions between 25 and 60%, as a function of the method and basis set. Using CCSD/d-aug-cc-pVTZ, the static vibrational counterpart amounts to 50% of the total anisotropy value whereas, at 1064 nm, it still represents one third of the total response.

For static quantities, the vibrational contribution is detrimental to the β_{SHS} amplitude. At the reference level, it amounts to -16% of the total value but it reaches as much as 50% at the HF and CCS levels. The impact of including vibrational contributions to the static DR_{SHS} depends strongly on the method and is rather negligible at the reference level. The situation is opposite for the dynamic β_{SHS} (at 1064 nm) since the vibrational contribution increases the response by about 10%. Again the relative vibrational counterpart gets larger at the HF and CCS levels. The contribution of the vibrations is modest on the dynamic DR_{SHS} , being of the order of -5%. Like for its static analog, changing the method leads to substantial variations of the vibrational contribution but, percentagewise, it remains small.

Finally, for γ_{THS} , at the reference level, the vibrational contribution amounts to 13% in the static limit and to 4% at 1064 nm. These are a rather small contributions, smaller than for the first hyperpolarizability. The vibrational contributions have a much larger effect on the static DR_{THS} and they lead to an increase by about 50%. The latter presents also a substantial dependence on the method and basis set. Note that owing to its large DR_{THS} values, γ_{THS} of the water molecule is typically dominated by its isotropic rather than by its

quadrupolar and hexadecapolar components. At 1064 nm, the vibrational contribution to DR_{THS} is small, of the same order of magnitude as the contribution to γ_{THS} .

These results have evidenced that the vibrational contributions to the dynamic α , β , and γ are small but not negligible, and non-systematic. Then, owing to the large effects of the method and basis set, it turns out that the CCSD/d-aug-cc-pVTZ level is mandatory for investigating the impact of vibrational contributions on the (hyper)polarizabilities of water.

Owing the larger computational cost of the vibrational contributions, a hybrid approach has been tested, where the electronic contribution is evaluated at the CCSD level, while the vibrational ones are calculated at the HF or CC2 levels of approximation (Table S9). If reliable, this hybrid method would be an efficient alternative to grasp most of the vibrational contributions. For instance, the resulting hybrid $\bar{\alpha}$ are in close agreement with the reference full CCSD value for the dynamic responses, and especially for the pure vibrational contributions, which are negligible. However, the differences amount to about 10% for the static $\Delta\alpha$. The agreement for the dynamic β is less good because of the differences between the ZPVA contributions, which can be larger than 50%. For instance, the vibrational contribution to the $\beta_{||}(-2\omega; \omega, \omega)$ response is overestimated by 50% at the CC2 level, raising question about the reliability of this hybrid scheme. On the other hand, the pure vibrational contribution are small for the dynamic responses. In the static limit, both the ZPVA and the pure vibrational contributions to the first hyperpolarizabilities varies substantially from one method to another. Finally, in the case the dynamic second hyperpolarizability, neither the HF, nor the CC2 method represent a good alternative to evaluate the vibrational contributions because the former underestimates these by about a factor of 3, while the latter underestimates it by more than a factor of 2. Again, the pure vibrational contributions are negligible.

TABLE II: Basis set and electron correlation effects on the total ($\alpha^e + \Delta\alpha^{ZPVA} + \alpha^{pv}$) static (top) and dynamic (bottom, 1064 nm) isotropic polarizability of water and its anisotropy. The amplitude of the vibrational counterpart (\mathcal{C}_v , %) is given in parentheses.

	HF	CCS	CC2	CCSD
		$\bar{\alpha}(0)$		
aug-cc-pVDZ	8.54 (6.7)	8.98 (6.5)	10.49 (5.6)	9.85 (5.5)
aug-cc-pVTZ	8.81 (6.6)	9.26 (6.4)	10.73 (5.6)	10.01 (5.5)
d-aug-cc-pVDZ	8.94 (6.6)	9.39 (6.4)	11.20 (5.5)	10.43 (5.4)
d-aug-cc-pVTZ	8.93 (6.6)	9.38 (6.4)	10.99 (5.6)	10.20 (5.5)
		$\Delta\alpha(0)$		
aug-cc-pVDZ	1.84 (26.9)	2.02 (25.0)	1.44 (27.2)	1.52 (26.2)
aug-cc-pVTZ	1.62 (34.2)	1.78 (31.5)	1.16 (42.8)	1.26 (39.1)
d-aug-cc-pVDZ	1.45 (39.5)	1.60 (35.9)	0.85 (58.0)	1.01 (49.5)
d-aug-cc-pVTZ	1.50 (39.0)	1.66 (35.5)	0.93 (61.4)	1.09 (50.6)
		$\bar{\alpha}(1064 \text{ nm})$		
aug-cc-pVDZ	8.23 (2.7)	8.67 (2.7)	10.30 (3.1)	9.64 (2.9)
aug-cc-pVTZ	8.49 (2.6)	8.93 (2.6)	10.52 (3.0)	9.78 (2.7)
d-aug-cc-pVDZ	8.62 (2.6)	9.07 (2.7)	11.01 (3.1)	10.23 (2.8)
d-aug-cc-pVTZ	8.61 (2.6)	9.06 (2.6)	10.78 (3.0)	9.97 (2.7)
		$\Delta\alpha(1064 \text{ nm})$		
aug-cc-pVDZ	1.59 (15.7)	1.78 (15.1)	1.27 (20.2)	1.35 (19.2)
aug-cc-pVTZ	1.30 (18.6)	1.47 (17.6)	0.87 (27.7)	0.99 (24.7)
d-aug-cc-pVDZ	1.11 (22.4)	1.28 (20.9)	0.56 (42.9)	0.74 (35.1)
d-aug-cc-pVTZ	1.15 (20.9)	1.32 (19.6)	0.55 (42.1)	0.75 (32.2)

TABLE III: Basis set and electron correlation effect on the total ($\beta^e + \Delta\beta^{ZPVA} + \beta^{pv}$) static (top) and dynamic (bottom, 1064 nm) SHS hyperpolarizability of water and of its depolarization ratio (DR). The amplitude of the vibrational counterpart (\mathcal{C}_v , %) is given in parentheses.

	HF	CCS	CC2	CCSD
$\beta_{SHS}(0)$				
aug-cc-pVDZ	5.28 (-42.7)	6.31 (-44.6)	12.42 (-20.0)	9.52 (-21.9)
aug-cc-pVTZ	4.96 (-51.0)	6.26 (-46.9)	13.75 (-16.0)	9.66 (-21.2)
d-aug-cc-pVDZ	4.11 (-51.8)	5.30 (-46.3)	12.64 (-10.1)	8.66 (-15.4)
d-aug-cc-pVTZ	4.47 (-51.3)	5.85 (-44.9)	14.32 (-10.1)	9.49 (-16.3)
$DR_{SHS}(0)$				
aug-cc-pVDZ	1.93 (-77.2)	2.38 (-76.3)	3.90 (-38.7)	3.24 (-50.6)
aug-cc-pVTZ	3.46 (-35.4)	4.32 (-30.2)	6.55 (-10.6)	5.76 (-16.1)
d-aug-cc-pVDZ	3.08 (-24.7)	4.00 (-21.9)	6.67 (-3.5)	5.52 (-15.4)
d-aug-cc-pVTZ	4.64 (-10.9)	5.64 (-10.0)	8.20 (-1.1)	7.55 (-2.4)
$\beta_{SHS}(1064 \text{ nm})$				
aug-cc-pVDZ	9.64 (18.4)	11.31 (16.1)	17.91 (10.7)	13.84 (10.6)
aug-cc-pVTZ	9.59 (17.9)	11.45 (16.0)	18.97 (9.4)	13.89 (9.9)
d-aug-cc-pVDZ	8.27 (20.4)	10.09 (19.2)	17.02 (10.1)	12.14 (10.9)
d-aug-cc-pVTZ	8.81 (18.8)	10.69 (16.6)	18.90 (8.9)	13.19 (9.5)
$DR_{SHS}(1064 \text{ nm})$				
aug-cc-pVDZ	3.71 (3.0)	3.96 (-11.5)	5.98 (-4.4)	5.30 (-5.6)
aug-cc-pVTZ	4.77 (-3.2)	5.62 (-5.3)	7.69 (-4.9)	6.96 (-5.9)
d-aug-cc-pVDZ	4.03 (0.7)	4.95 (-2.4)	7.07 (-4.7)	6.15 (-3.9)
d-aug-cc-pVTZ	5.09 (-5.3)	6.05 (-6.9)	8.43 (-3.5)	7.76 (-5.8)

TABLE IV: Basis set and electron correlation effect on the total ($\gamma^e + \Delta\gamma^{ZPVA} + \gamma^{pv}$) static (top) and dynamic (bottom, 1064 nm) THS hyperpolarizability of water and of its depolarization ratio (DR). The amplitude of the vibrational counterpart (\mathcal{C}_v , %) is given in parentheses.

	HF	CCS	CC2	CCSD
$\gamma_{THS}(0)$				
aug-cc-pVDZ	759 (22.2)	885 (21.4)	1690 (18.8)	1303 (18.2)
aug-cc-pVTZ	910 (20.2)	1064 (19.2)	2012 (16.8)	1506 (16.3)
d-aug-cc-pVDZ	1103 (17.2)	1274 (16.5)	2871 (14.5)	2084 (13.6)
d-aug-cc-pVTZ	1190 (16.3)	1371 (15.7)	2938 (14.0)	2101 (13.3)
$DR_{THS}(0)$				
aug-cc-pVDZ	660 (70.0)	699 (64.3)	309 (66.9)	416 (71.8)
aug-cc-pVTZ	1465 (88.0)	1820 (88.4)	290 (65.5)	417 (72.7)
d-aug-cc-pVDZ	312 (74.0)	380 (74.9)	100 (46.9)	126 (53.5)
d-aug-cc-pVTZ	411 (74.9)	504 (76.2)	127 (46.8)	166 (54.3)
$\gamma_{THS}(1064 \text{ nm})$				
aug-cc-pVDZ	728 (4.2)	792 (-2.9)	1904 (5.3)	1406 (3.9)
aug-cc-pVTZ	891 (3.9)	976 (-2.9)	2276 (5.3)	1635 (3.9)
d-aug-cc-pVDZ	1127 (3.5)	1301 (3.5)	3486 (6.1)	2402 (4.1)
d-aug-cc-pVTZ	1226 (3.6)	1410 (3.6)	3497 (6.0)	2387 (4.2)
$DR_{THS}(1064 \text{ nm})$				
aug-cc-pVDZ	132 (22.4)	68 (-81.6)	38 (0.9)	50 (5.6)
aug-cc-pVTZ	128 (20.6)	178 (32.3)	46 (1.3)	60 (5.7)
d-aug-cc-pVDZ	69 (14.5)	80 (14.9)	32 (0.6)	39 (3.7)
d-aug-cc-pVTZ	86 (13.9)	99 (14.3)	42 (0.7)	51 (3.8)

C. Frequency dispersion and decomposition into the different vibrational contributions

Now, we focus on the impact of each vibrational contribution to the total value and we describe their frequency dispersions. The results are listed in Tables V-VII. Additional details are provided in Tables S2-S4 where the independent non-zero tensor components are listed.

Like its electronic counterpart, the ZPVA contribution to the isotropic polarizability increases slightly with the optical frequency. From 694 nm to the static limit, it amounts to roughly 3%. The mechanical anharmonicity contributes the most to the (first order) ZPVA correction, in a 2:1 ratio with respect to the electrical anharmonicity term. The pure vibrational term has, in the static limit, a similar amplitude to the ZPVA correction but it drops strongly in the dynamic regime. Note that the harmonic term is the main pure vibrational contribution, much larger than the second-order anharmonicity term. For the polarizability anisotropy, in the static limit the ZPVA correction and pure vibrational term are again of the same order of magnitude but in the dynamic regime the ZPVA term dominates again the whole vibrational response. Moreover, the mechanical anharmonicity term is also the largest and about twice bigger than the electrical anharmonicity one. The frequency dispersion of the harmonic term is characterized by a decrease of its amplitude with the frequency (like for the isotropic average) whereas the second-order anharmonic term presents a non-monotonic frequency dispersion, due a resonance in those terms, between the optical frequency and the sum of the two stretching vibrational frequencies close to 1300 nm. Analyzing the tensor components (Table S2), the largest static and dynamic ZPVA component is α_{yy} and, in the static limit, α^{pv} is determined by the α_{zz} component. Note that there is no pure vibrational contribution to α_{xx} since, $\forall a, \left(\frac{\partial \mu_x}{\partial Q_a}\right)_0 = 0$.

The frequency dispersion of the first hyperpolarizability presents similarities to that of the polarizability, though it is naturally exalted owing to its SHG character. The ZPVA correction evolves smoothly with the frequency, as does the electronic contribution. Again, the mechanical anharmonicity term is the largest, with a 3:1 ratio with respect to the electrical anharmonicity. In the pure vibrational contribution, the $[\mu\alpha]^0$ harmonic term is the largest, followed by $[\mu\alpha]^{\text{II}}$, and they both fade out when the optical frequency increases. On the other hand, the static β^{pv} is much larger than the dynamic one. It is of the opposite sign

TABLE V: Electronic and vibrational contributions to the average polarizability and polarizability anisotropy as computed at the CCSD/d-aug-cc-pVTZ level at different wavelengths.

	Total	Electronic	ZPVA			Pure vibrational			
			$\mathcal{C}_{[\alpha]^{1,0}}$	$\mathcal{C}_{[\alpha]^{0,1}}$	\mathcal{C}_{ZPVA}	$\mathcal{C}_{[\mu^2]^0}$	$\mathcal{C}_{[\mu^2]^{\text{II}}}$	\mathcal{C}_{pv}	\mathcal{C}_v
				$\bar{\alpha}$					
∞	10.20	9.64	0.9	1.9	2.8	2.8	-0.1	2.7	5.5
1500 nm	9.92	9.67	0.9	2.0	2.9	-0.4	0.0	-0.3	2.6
1300 nm	9.96	9.68	0.9	2.0	2.9	-0.3	0.2	-0.1	2.8
1064 nm	9.97	9.70	0.9	2.0	2.9	-0.2	0.0	-0.2	2.7
694.3 nm	10.08	9.79	0.9	2.0	2.9	-0.1	0.0	-0.1	2.9
				$\Delta\alpha$					
∞	1.09	0.54	7.9	12.1	19.6	25.6	-1.1	26.7	50.6
1500 nm	0.74	0.52	12.9	22.0	34.8	-6.4	1.1	-5.3	29.7
1300 nm	0.78	0.52	12.3	20.9	33.1	-4.0	4.7	0.7	34.0
1064 nm	0.75	0.51	13.0	21.9	34.8	-2.5	-0.3	-2.7	32.2
694.3 nm	0.72	0.47	13.7	22.8	36.3	-0.9	0.0	-1.0	35.4

to the electronic counterpart and it dominates the vibrational response. The inclusion of vibrational contributions modifies DR_{SHS} by at most 10% with a non-monotonic frequency dispersion that originates from the pure vibrational (harmonic) contribution. The amplitudes of the three non-zero independent $\beta^e(0; 0, 0)$ tensor components (Table S3) satisfy the $\beta_{xxz} < \beta_{yyz} < \beta_{zzz}$ ordering. The pure vibrational contribution is also dominated by β_{zzz} , followed by β_{zyy} , which are much larger than β_{zxx} . For these dominant tensor components, contrary to the electronic and ZPVA contributions, the harmonic contribution to β^{pv} is positive but it is partly canceled by the $[\mu^3]^{\text{I}}$ first-order anharmonic term. On the other hand, for the ZPVA correction, the largest component is β_{yyz} , followed by β_{zzz} , and both are also much larger than β_{xxz} . The small $\beta_{(xxz)}$ contributions are again explained by the zero $\left(\frac{\partial \mu_x}{\partial Q_a}\right)_0$ quantities. For both β^e and $\Delta\beta^{ZPVA}$, these relative amplitudes remain when considering the dynamic responses, with small differences between the Kleinman-related tensor components

TABLE VI: Electronic and vibrational contributions to the SHS first hyperpolarizability and DR as computed at the CCSD/d-aug-cc-pVTZ level at different wavelengths.

	Total	Electronic	ZPVA			Pure vibrational				
			$\mathcal{C}_{[\beta]^1,0}$	$\mathcal{C}_{[\beta]^0,1}$	\mathcal{C}_{ZPVA}	$\mathcal{C}_{[\mu\alpha]^0}$	$\mathcal{C}_{[\mu\alpha]^{\text{II}}}$	$\mathcal{C}_{[\mu^3]^{\text{I}}}$	\mathcal{C}_{pv}	\mathcal{C}_v
β_{SHS}										
∞	9.49	11.04	1.9	5.8	7.6	-36.1	-5.2	15.5	-24.2	-16.3
1500 nm	13.22	11.47	1.6	4.5	6.1	8.3	-1.2	0.1	7.2	13.2
1300 nm	12.91	11.62	1.7	4.7	6.3	5.7	-2.0	0.0	3.7	10.0
1064 nm	13.19	11.93	1.7	4.7	6.4	3.4	-0.2	0.0	3.2	9.5
694.3 nm	14.51	13.37	2.0	4.8	6.8	1.2	-0.1	0.0	1.1	7.9
DR_{SHS}										
∞	7.55	7.73	-0.9	-1.5	-2.3	-7.6	1.0	17.7	0.7	-2.4
1500 nm	7.26	7.96	-1.0	-1.8	-2.8	-6.6	0.2	0.1	-6.2	-9.6
1300 nm	7.30	8.04	-1.0	-1.8	-2.8	-4.3	-2.2	0.0	-6.6	-10.0
1064 nm	7.76	8.21	-1.1	-1.9	-3.0	-2.6	0.1	0.0	-2.6	-5.8
694.3 nm	8.72	9.06	-1.0	-1.9	-2.8	-1.0	0.0	0.0	-1.0	-3.9

[e.g. $\beta_{x(xz)}$ and β_{zxx}]. Finally, it is interesting to note that, at 1064 nm, deviations with respect to Kleinman's conditions are much larger for the pure vibrational contribution than for the ZPVA correction. Indeed, if one compares e.g. the β_{zyy} and β_{yyz} components, the difference attains 22 % at 1064 nm for $[\mu\alpha]^0$, while 0.6 % for $\Delta\beta^{ZPVA}$.

The ZPVA correction to γ_{THS} increases with the frequency, from 4 % in the static limit to 6 % at 694.3 nm (Table VII). Again, it is dominated by the mechanical anharmonicity term, though the electrical anharmonicity term increases faster with the frequency. The pure vibrational contributions to γ_{THS} are small, even in the static limit where it attains only 10 %. At optical frequency, the whole γ^{pv} as well as any of its components contribute to less than 1 % and can therefore be considered negligible. Note that the largest contribution to γ^{pv} comes from the $[\alpha^2]^0$ Raman term. Vibrational contributions are larger on DR_{THS} , in particular for the static value, which is strongly enhanced by the harmonic $[\alpha^2]^0$ and $[\mu\beta]^0$ terms. At optical frequencies, the pure vibrational contribution to DR_{THS} is small

whereas its ZPVA correction is slightly larger. At 694.3 nm, both vibrational contributions are strongly reduced. Contrary to the lower-order properties, the largest electronic component (in amplitude) is γ_{xxxx} , then γ_{zzzz} and γ_{yyyy} (Table S4). In the static limit, the dominant tensor components to γ^{pv} satisfy the following ordering: $\gamma_{yyyy} > \gamma_{zzzz} > \gamma_{yyzz}$ whereas for the ZPVA correction it is $\gamma_{xxxx} > \gamma_{yyyy} > \gamma_{zzzz}$. Owing to their negligible values, the $\gamma^{pv}(-3\omega; \omega, \omega, \omega)$ tensor components are not discussed. For $\Delta\gamma^{ZPVA}(-3\omega; \omega, \omega, \omega)$ γ_{xxxx} is still the largest component whereas the amplitudes of the two other diagonal components are in reverse order. For those components that satisfy Kleinman's conditions in the static limit, the differences amount to about 10 % for the electronic and pure vibrational contributions while it can be twice larger for the ZPVA correction.

TABLE VII: Electronic and vibrational contributions to the THS second hyperpolarizability and DR as computed at the CCSD/d-aug-cc-pVTZ level at different wavelengths.

	Total	Electronic	ZPVA			Pure vibrational							
			$C_{[\gamma]^{1,0}}$	$C_{[\gamma]^{0,1}}$	C_{ZPVA}	$C_{[e^2]^0}$	$C_{[e^2]^H}$	$C_{[\mu\beta]^0}$	$C_{[\mu\beta]^H}$	$C_{[\mu^2\alpha]^1}$	$C_{[\mu^4]^H}$	C_{pv}	C_v
∞	2101	1821	1.1	2.5	3.5	7.3	1.7	-0.5	0.0	0.9	0.5	9.8	13.3
1500nm	2108	2033	1.3	2.8	4.1	-0.6	0.0	0.1	0.0	0.0	0.0	-0.5	3.6
1300nm	2195	2113	1.3	2.9	4.2	-0.4	0.0	0.1	0.0	0.0	0.0	-0.4	3.8
1064nm	2387	2288	1.4	3.0	4.4	-0.3	0.0	0.0	0.0	0.0	0.0	-0.2	4.2
694.3nm	3622	3401	2.4	3.8	6.2	-0.1	0.0	0.0	0.0	0.0	0.0	-0.1	6.1
γ_{THS}													
∞	166	76	4.7	1.6	6.3	42.3	13.3	-5.1	-0.9	5.9	3.0	50.7	54.3
1500nm	64	61	3.9	2.3	6.2	-3.9	-0.2	1.7	-0.1	0.0	0.0	-2.3	4.0
1300nm	60	57	3.7	2.0	5.8	-2.7	-0.2	1.1	-0.1	0.0	0.0	-1.8	4.1
1064nm	51	49	3.3	1.5	4.8	-1.5	-0.1	0.6	0.0	0.0	0.0	-1.1	3.8
694.3nm	23	24	-0.4	-1.3	-1.8	-0.3	0.0	0.1	0.0	0.0	0.0	-0.2	-2.1
DR_{THS}													

D. Contributions of the vibrational normal modes

An analysis of the vibrational normal mode contributions is provided in Fig. 2 as well as in Table S5. At 1064 nm, the symmetric stretching vibration contributes most to the linear and nonlinear optical responses, followed by the antisymmetric stretching and finally the bending mode. In the static limit, the percentage contributions of modes 2 and 3 change but mode 2 still provides larger contributions than mode 3. On the other hand, for $\bar{\alpha}$ and β_{SHS} , the bending mode contributes substantially with contributions of the same ($\bar{\alpha}$) or opposite (β_{SHS}) signs. In details, on the one hand, the large cubic force constant of the A_1 stretching explains the large $[\chi^{(3)}]^{0,1}$ contributions in both the static and dynamic cases. On the other hand, a large $\left(\frac{\partial \mu_z}{\partial Q_1}\right)_0$ is at the origin of the large P^{pv} contributions of the A_1 bending mode, in the static case.

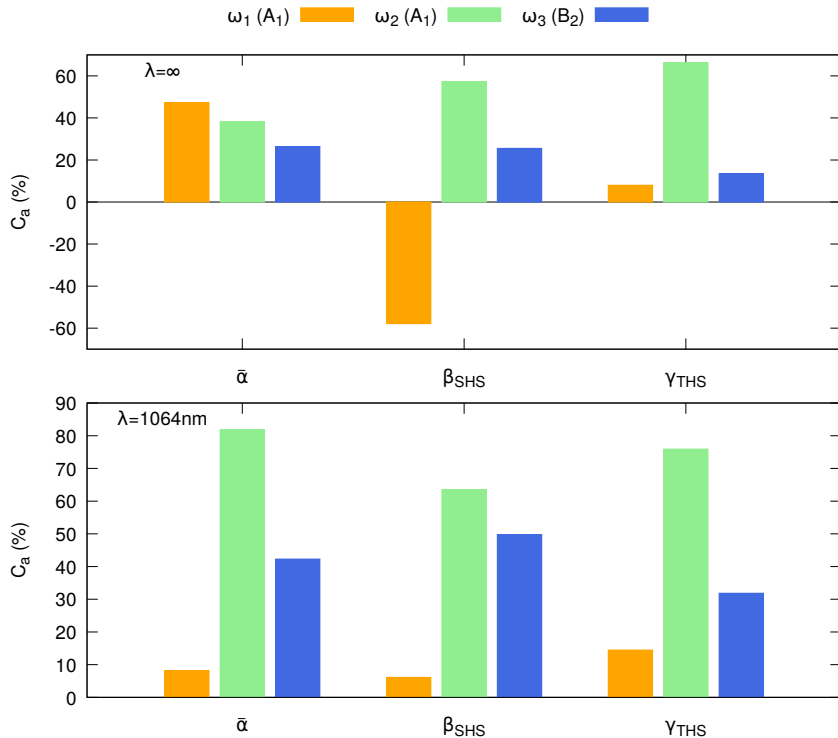


FIG. 2: Missing mode analysis [C_a , %] (ω_1 , A_1 bending; ω_2 , A_1 symmetric stretching; ω_3 , B_2 antisymmetric stretching) to the static (top) and dynamic ($\lambda = 1064$ nm, bottom) total vibrational contributions to $\bar{\alpha}$, β_{SHS} , and γ_{THS}), as computed at the CCSD/d-aug-cc-pVTZ level.

E. Comparison with other theoretical investigations

Comparisons with previous works focusing on the whole responses and their contributions are given in Tables VIII (polarizability) and IX (first and second hyperpolarizabilities). A selection of additional data are listed in Tables S6-S8 for the electronic counterpart. In the case of the vibrational responses, in order to provide a more detailed comparison between levels of approximation, in Table IX, the more common (static and dynamic) $\beta_{||}(-2\omega; \omega, \omega)$ quantity is considered instead of β_{SHS} while γ_{THS} is replaced by the static $\gamma_{||}$ since no dynamic third harmonic γ values were available. Note that in several cases, the listed quantities were calculated from the different tensor components reported in the corresponding original investigations.

The analysis of the electronic contributions (Tables S6-S8) reminds several known or less known effects, including (i) basis set effects are stronger for computing the hyperpolarizabilities than the polarizability, (ii) the impact of the triple excitations is rather small, as estimated by comparison with the CCSD(T) results of Maroulis⁸⁹ and the CC3 ones due to Christiansen⁸⁰, (iii) electron correlation effects are large and increase with the order of the response, (iv) the MP2 approach provides a good agreement with higher-level calculations (though this agreement worsens at the MP3 and MP4 levels) and the QED-MP2 method of Kobayashi *et al.*^{90,91} quantitatively reproduces the frequency dispersion of the first hyperpolarizability, (v) the MR-CI approach of Spelsberg *et al.*⁹² slightly overestimates the first hyperpolarizabilities, (vi) most reported DFT results overestimate the molecular responses and their frequency dispersion, though the use of hybrid exchange-correlation functionals (like mPW91PW91) improves the agreement and the exact exchange functional formalism of Bokhan and Bartlett⁹³ gives results close to the Hartree-Fock ones, (vii) these limitations of DFT with conventional exchange-correlation functionals are exalted in the case of the higher-order response properties,

The first reports on the ZPVA contributions to the polarizability of the water molecule⁹⁴⁻⁹⁷ have employed the HF level and the POL basis set.⁹⁸ They predict that, in the static limit, $\Delta\alpha^{ZPVA}$ amounts to a few percents of the electronic polarizability (3 %) and that it increases by less than one percent at 694.3 nm, which whom values are in good agreement with more recent correlated results, thought slightly smaller (15 %). In the case of the polarizability anisotropy, the HF values are typically 25 % larger than at the CCSD level. Moreover, the

ZPVA contributions to the polarizability as estimated at the MP2 level by Cohen *et al.*⁹⁹ after including higher-order derivatives are similar to those obtained using the sum of the two first contributions, $[\alpha]^{1,0} + [\alpha]^{0,1}$. In the case of the first hyperpolarizability, the HF ZPVA values are larger than those obtained at correlated (MP2 and CCSD) levels so that their relative contribution to the total first hyperpolarizability increases by about a factor of two since, at the same time, the electronic contributions are underestimated. We note also that there is a nice consistency between the MP2 and CCSD $\Delta\alpha^{ZPVA}$ and $\Delta\beta^{ZPVA}$ values while the MP2/POL $\Delta\gamma^{ZPVA}$ values are smaller than the CCSD/d-aug-cc-pVTZ results, by about 30%. The agreement between the vibrational CI results of Christiansen and co-workers^{100–103} and ours, for the polarizability, first and second hyperpolarizabilities, employing the same electronic structure method, is excellent.

Considering now the pure vibrational counterpart, Bishop *et al.*¹⁰⁴ already reported in 1993 its contributions to the first and second hyperpolarizabilities of the water molecule (without the $[\mu\alpha]^{0,2}$ and $[\mu^4]^{0,2}$ terms). In the static limit, they found that the HF \mathcal{C}_{pv} values attain as much as 47% (17%) for the first (second) hyperpolarizabilities, and that these percentages decrease to 11% (16%) at the MP2 level. Later,¹⁰⁵ they detailed the different contributions to the second hyperpolarizability tensor at the HF level, and pinpointed the importance of the $[\alpha^2]$ term over the other ones. Moreover, Cohen *et al.*⁹⁹ investigated the impact of the third-order derivatives of μ to the pv contributions and found it to be small. Also, the nuclear relaxation approach due to Luis *et al.*⁹⁵ predicted very similar results to those obtained with perturbation theory. Static MP2 results have later been calculated by Reis *et al.*¹⁰⁶, showing that the pure vibrational contribution amounts to 3% of the polarizability, 27% of the first hyperpolarizability (note that the difference with respect to Ref. 104 can be explained by the inclusion of the $[\mu\alpha]^{0,2}$ term) and 13% of the second hyperpolarizability (in close agreement with our results). More recently, Thorvaldsen *et al.*¹⁰⁷ studied the impact of the basis set on the HF vibrational contributions (only including the so-called double harmonic, $m=n=0$ terms) and advocated the use of d-aug-cc-pVTZ or POL. Finally, the VCI approach of Christiansen and co-workers¹⁰² provides similar results to those of the present study in the static limit as well as for the SHS first hyperpolarizability at 694.3 nm.

TABLE VIII: α^e , $\Delta\alpha^{ZPVA}$, and α^{pv} contributions to the static and dynamic (at 694.3 nm) isotropic polarizability ($\bar{\alpha}$, a.u.) and polarizability anisotropy ($\Delta\alpha$, a.u.) of the water molecule, as calculated at different levels of approximation.

Method	Basis set	Frequency	Contributions			Reference
			P^e	ΔP^{ZPVA}	P^{pv}	
$\bar{\alpha}(-\omega; \omega)$						
HF	POL	static	—	0.247	—	94
HF	POL	static	—	0.247	0.333	95
HF	POL	static	8.362	0.247	—	96
HF	POL	694.3 nm	8.461 ^a	0.266 ^a	—	96
HF	d-aug-cc-pVTZ	static	8.602	—	0.378	107
MP2	POL	static	—	0.292	—	94
MP2	POL	static	9.944	0.292	0.286	106
CCSD + VCI	d-aug-cc-pVTZ	static	9.638	0.285	0.295	100 and 101
CCSD	d-aug-cc-pVTZ	static	9.638	0.286	0.276	This work
CCSD + VCI	d-aug-cc-pVTZ	694.3 nm	9.788	0.296	-0.006	100 and 101
CCSD	d-aug-cc-pVTZ	694.3 nm	9.788	0.296	-0.006	This work
$\Delta\alpha(-\omega; \omega)$						
HF	POL	static	—	0.268	—	94
HF	POL	static	—	0.268	0.348	95
MP2	POL	static	—	0.242	—	94
MP2 ^c	POL	static	0.527	0.242	0.722	106
CCSD + VCI	d-aug-cc-pVTZ	static	0.537	0.265	0.743	100 and 101
CCSD	d-aug-cc-pVTZ	static	0.536	0.262	0.664	This work
CCSD + VCI	d-aug-cc-pVTZ	694.3 nm	0.467	0.270	0.009	100 and 101
CCSD	d-aug-cc-pVTZ	694.3 nm	0.466	0.264	0.009	This work

^a Interpolated using the frequency dispersion.

TABLE IX: Static (and dynamic, at 694.3 nm) electronic, ZPVA, and pure vibrational contributions to $\beta_{||}(-2\omega; \omega, \omega)$ and $\gamma_{||}$ (in a.u.) of the water molecule, as calculated at different levels of approximation.

Method	Basis set	Frequency	Contributions			Reference
			P^e	ΔP^{ZPVA}	P^{pv}	
$\beta_{ }(-2\omega; \omega, \omega)$						
HF	POL	static	—	—	3.983	104
HF	POL	static	—	-1.397	4.141	95
HF	POL	static	-7.53	-1.397	—	97
HF	POL	694.3 nm	-8.97 ^a	-1.687 ^a	—	97
HF	d-aug-cc-pVTZ	static	-11.01	—	9.351	107
MP2	POL	static	—	—	1.472	104
MP2	POL	static	-13.59	-0.95	3.73	106
CCSD + VCI	d-aug-cc-pVTZ	static	-17.70	-1.039	2.645	102
CCSD	d-aug-cc-pVTZ	static	-17.70	-1.101	3.647	This work
CCSD + VCI	d-aug-cc-pVTZ	694.3 nm	-21.68	-1.438	-0.243	102
CCSD	d-aug-cc-pVTZ	694.3 nm	-21.68	-1.488	-0.237	This work
$\gamma_{ }$						
HF	POL	static	—	—	150.1	104 and 105
HF	POL	static	—	—	148.9	95
HF	d-aug-cc-pVTZ	static	999	—	144.6	107
MP2	POL	static	1400	—	235.2	50 and 104
MP2	POL	static	1447	51	187	106
CCSD + VCI	d-aug-cc-pVTZ	static	1736	75.8	171.6	103
CCSD	d-aug-cc-pVTZ	static	1745	75.6	240.4	This work

^a Interpolated using the frequency dispersion expressions.

V. CONCLUSIONS

Second harmonic scattering (SHS) first hyperpolarizability (β_{SHS}) and third harmonic scattering (THS) second hyperpolarizability (γ_{THS}) are all-optical nonlinear optical processes. For such processes, theoretical models predict that the pure vibrational contributions are small while the zero-point vibrational averages (ZPVA) are modest, which explains why they are neglected in most quantum chemical investigations. In addition, THS has mostly been ignored until the last three years and the publication of two experimental papers.^{6,7} This gives the incentive for investigating, by employing quantum chemistry methods, the vibrational contributions to SHS and THS of the water molecule and for comparing these to their electronic counterparts. Thus, this paper has reported on the vibrational contributions to the average polarizability ($\bar{\alpha}$), to β_{SHS} and its depolarization ratio (DR_{SHS}), as well as to γ_{THS} and its depolarization ratio (DR_{THS}) by using the Bishop and Kirtman perturbative theory approach in combination with finite differentiation techniques to evaluate the higher-order derivatives. This has been performed by employing a hierarchy of Coupled Clusters techniques and extended atomic basis sets, from which the CCSD/d-aug-cc-pVTZ level has been selected to assess the importance of the ZPVA contributions and of the pure vibrational contributions with respect to their electronic counterparts. Numerical results on the water molecules highlight that i) the vibrational contributions to the dynamic $\bar{\alpha}$, β_{SHS} , and γ_{THS} are small but still not negligible, ii) they amount to respectively 3, 10, and 4% at the typical wavelength of 1064 nm, iii) the mechanical anharmonicity term dominates the zero-point vibrational average (ZPVA) contribution, iv) the double harmonic terms dominate the pure vibrational contributions, v) the stretching vibrations provide the largest contributions to the dynamic (hyper)polarizabilities, and vi) these conclusions are strongly impacted in the static limit where the vibrational contributions are much larger, in particular the double harmonic pure vibrational terms, and even more in the case of β_{SHS} . It was further interesting to observe that the relative vibrational contributions to the optical responses do not increase with the order of the response. Still, confirmations about their absolute and relative amplitudes deserve investigating other compounds, from small reference systems like those studied in Ref. 74 to NLO active molecules like (push-pull) π -conjugated molecules.

Appendix A: Non-zero components of the tensors

Owing to the C_{2v} symmetry of the water molecule, group theory^{72,108} ensures that

$$\left(\frac{\partial\mu_i}{\partial Q_a}\right)_0 \begin{cases} \neq 0 & \text{if } Q_a \text{ belongs to } A_1 \text{ and } i = z. \\ \neq 0 & \text{if } Q_a \text{ belongs to } B_2 \text{ and } i = y. \\ = 0 & \text{otherwise.} \end{cases} \quad (\text{A1})$$

$$\left(\frac{\partial\alpha_{ij}}{\partial Q_a}\right)_0 \begin{cases} \neq 0 & \text{if } Q_a \text{ belongs to } A_1 \text{ and } ij = xx, yy \text{ or } zz. \\ \neq 0 & \text{if } Q_a \text{ belongs to } B_2 \text{ and } ij = (yz). \\ = 0 & \text{otherwise.} \end{cases} \quad (\text{A2})$$

$$\left(\frac{\partial\beta_{ijk}}{\partial Q_a}\right)_0 \begin{cases} \neq 0 & \text{if } Q_a \text{ belongs to } A_1 \text{ and } ijk = x(xz), y(yz), zxx, zyy, zzz. \\ \neq 0 & \text{if } Q_a \text{ belongs to } B_2 \text{ and } ijk = x(xy), yxx, yzz, yyy, z(zy). \\ = 0 & \text{otherwise.} \end{cases} \quad (\text{A3})$$

$$\left(\frac{\partial\gamma_{ijkl}}{\partial Q_a}\right)_0 \begin{cases} \neq 0 & \text{if } Q_a \text{ belongs to } A_1 \text{ and } ijkl = xxxx, x(xyy), x(xzz), y(xxy), \\ & \text{yyyy, } y(yzz), z(xxz), z(yyz), zzzz. \\ \neq 0 & \text{if } Q_a \text{ belongs to } B_2 \text{ and } ijkl = x(xyz), y(xxz), y(yyz), yzzz, \\ & z(xxy), zyyy, z(yzz). \\ = 0 & \text{otherwise.} \end{cases} \quad (\text{A4})$$

Additionally,

$$\left(\frac{\partial^2 P}{\partial Q_a \partial Q_b}\right)_0 \in \begin{cases} A_1 & \text{if } Q_a \text{ and } Q_b \text{ are } A_1 \text{ modes,} \\ A_1 & Q_a = Q_b \text{ is the } B_2 \text{ mode,} \\ B_2 & \text{otherwise.} \end{cases} \quad (\text{A5})$$

So that, out of the 9 second-order derivatives, 5 belong to the A_1 irreducible representation (irrep) and 4 to the B_2 irrep. The non-zero components are thus the same as the first-order ones, for the corresponding P and irrep.

ACKNOWLEDGMENTS

The calculations were performed on the computers of the Consortium des Équipements de Calcul Intensif, including those of the Technological Platform of High-Performance Computing, for which we gratefully acknowledge the financial support of the FNRS-FRFC, of the Walloon Region, and of the University of Namur (Conventions No. 2.5020.11, GEQ U.G006.15, 1610468, and RW/GEQ2016).

REFERENCES

- ¹G. H. Wagnière, *Linear and Nonlinear Optical Properties of Molecules* (Helv. Chim. Acta, Basel, 1993) oCLC: 246731393.
- ²C. Bosshard, *Organic Nonlinear Optical Materials* (Gordon and Breach, Basel, Switzerland, 1995) oCLC: 33261662.
- ³M. G. Papadopoulos, A. J. Sadlej, and J. Leszczynski, *Non-Linear Optical Properties of Matter From Molecules to Condensed Phases* (Springer, Dordrecht, 2006) oCLC: 762167749.
- ⁴T. Verbiest, K. Clays, and V. Rodriguez, *Second-Order Nonlinear Optical Characterization Techniques: An Introduction* (Taylor & Francis, 2009).
- ⁵K. Clays and A. Persoons, Phys. Rev. Lett. **66**, 2980 (1991).
- ⁶N. Van Steerteghem, K. Clays, T. Verbiest, and S. Van Cleuvenbergen, Anal. Chem. **89**, 2964 (2017).
- ⁷V. Rodriguez, J. Phys Chem. C **121**, 8510 (2017).
- ⁸S. R. Marder, L.-T. Cheng, B. G. Tiemann, A. C. Friedli, M. Blanchard-Desce, J. W. Perry, and J. Skindhøj, Science **263**, 511 (1994).
- ⁹J. Zyss and I. Ledoux, Chem. Rev. **94**, 77 (1994).
- ¹⁰J. L. Brédas, C. Adant, P. Tackx, A. Persoons, and B. M. Pierce, Chem. Rev. **94**, 243 (1994).
- ¹¹D. R. Kanis, M. A. Ratner, and T. J. Marks, Chem. Rev. **94**, 195 (1994).
- ¹²X. Hu, D. Xiao, S. Keinan, I. Asselberghs, M. J. Therien, K. Clays, W. Yang, and D. N. Beratan, J. Phys Chem. C **114**, 2349 (2010).

- ¹³N. H. List, R. Zaleśny, N. A. Murugan, J. Kongsted, W. Bartkowiak, and H. Ågren, J. Chem. Theory Comput. **11**, 4182 (2015).
- ¹⁴D. P. Shelton and J. E. Rice, Chem. Rev. **94**, 3 (1994).
- ¹⁵T. Kobayashi, K. Sasagane, F. Aiga, and K. Yamaguchi, J. Chem. Phys. **111**, 842 (1999).
- ¹⁶G. Maroulis, Chem. Phys. Lett. **442**, 265 (2007).
- ¹⁷R. J. Wheatley, J. Comput. Chem. **29**, 445 (2008).
- ¹⁸P. Norman, Phys. Chem. Chem. Phys. **13**, 20519 (2011).
- ¹⁹J. P. Coe and M. J. Paterson, J. Chem. Phys. **141**, 124118 (2014).
- ²⁰D. M. Bishop, Int. Rev. Phys. Chem. **13**, 21 (1994).
- ²¹B. Champagne and D. M. Bishop, in *Advances in Chemical Physics* (John Wiley & Sons, Ltd, 2003) pp. 41–92.
- ²²J. Kongsted, A. Osted, K. V. Mikkelsen, and O. Christiansen, J. Chem. Phys. **120**, 3787 (2004).
- ²³T. Seidler, K. Stadnicka, and B. Champagne, J. Chem. Phys. **139**, 114105 (2013).
- ²⁴E. Mishina, Y. Miyakita, Q.-K. Yu, S. Nakabayashi, and H. Sakaguchi, The Journal of Chemical Physics **117**, 4016 (2002).
- ²⁵C. Tonnelé, K. Pielak, J. Deviers, L. Muccioli, B. Champagne, and F. Castet, Phys. Chem. Chem. Phys. **20**, 21590 (2018).
- ²⁶B. E. K. Dalskov, H. J. A. Jensen, and J. Oddershede, Mol. Phys. **90**, 3 (1997).
- ²⁷M. de Wergifosse, F. Castet, and B. Champagne, J. Chem. Phys. **142**, 194102 (2015).
- ²⁸R. Zaleśny, I. W. Bulik, W. Bartkowiak, J. M. Luis, A. Avramopoulos, M. G. Papadopoulos, and P. Krawczyk, J. Chem. Phys. **133**, 244308 (2010).
- ²⁹A. S. Dutra, M. A. Castro, T. L. Fonseca, E. E. Fileti, and S. Canuto, J. Chem. Phys. **132**, 034307 (2010).
- ³⁰V. Lacivita, M. Rérat, B. Kirtman, R. Orlando, M. Ferrabone, and R. Dovesi, J. Chem. Phys. **137**, 014103 (2012).
- ³¹I. W. Bulik, R. Zaleśny, W. Bartkowiak, J. M. Luis, B. Kirtman, G. E. Scuseria, A. Avramopoulos, H. Reis, and M. G. Papadopoulos, J. Comput. Chem. **34**, 1775 (2013).
- ³²B. Gao, M. Ringholm, R. Bast, K. Ruud, A. J. Thorvaldsen, and M. Jaszuński, J. Phys. Chem. A **118**, 748 (2014).
- ³³E. S. Naves, M. A. Castro, and T. L. Fonseca, Chem. Phys. Lett. **608**, 130 (2014).

- ³⁴R. Zaleśny, A. Baranowska-Łączkowska, M. Medved', and J. M. Luis, *J. Chem. Theory Comput.* **11**, 4119 (2015).
- ³⁵E. S. Naves, M. A. Castro, and T. L. Fonseca, *J. Chem. Phys.* **134**, 054315 (2011).
- ³⁶E. S. Naves, M. A. Castro, and T. L. Fonseca, *J. Chem. Phys.* **136**, 014303 (2012).
- ³⁷R. Zaleśny, M. Garcia-Borràs, R. W. Góra, M. Medved', and J. M. Luis, *Phys. Chem. Chem. Phys.* **18**, 22467 (2016).
- ³⁸S. Marques, M. A. Castro, S. A. Leão, and T. L. Fonseca, *J. Phys. Chem. A* **122**, 7402 (2018).
- ³⁹M. Garcia-Borràs, M. Solà, J. M. Luis, and B. Kirtman, *J. Chem. Theory Comput.* **8**, 2688 (2012).
- ⁴⁰L. Feitoza, M. A. Castro, S. A. Leão, and T. L. Fonseca, *J. Chem. Phys.* **146**, 144309 (2017).
- ⁴¹S. Casassa, J. Baima, A. Mahmoud, and B. Kirtman, *J. Chem. Phys.* **140**, 224702 (2014).
- ⁴²L. Z. Kang, T. Inerbaev, B. Kirtman, and F. L. Gu, *Theor. Chem. Acc.* **130**, 727 (2011).
- ⁴³A. Avramopoulos, H. Reis, N. Otero, P. Karamanis, C. Pouchan, and M. G. Papadopoulos, *J. Phys. Chem. C* **120**, 9419 (2016).
- ⁴⁴M. Torrent-Sucarrat, S. Navarro, E. Marcos, J. M. Anglada, and J. M. Luis, *J. Phys. Chem. C* **121**, 19348 (2017).
- ⁴⁵G. Avila, *J. Chem. Phys.* **122**, 144310 (2005).
- ⁴⁶G. D. Purvis and R. J. Bartlett, *Phys. Rev. A* **23**, 1594 (1981).
- ⁴⁷D. M. Bishop and J. Pipin, *Theor. Chem. Acc* **71**, 247 (1987).
- ⁴⁸A. V. Gubskaya and P. G. Kusalik, *Mol. Phys.* **99**, 1107 (2001).
- ⁴⁹D. M. Bishop and B. Lam, *Phys. Rev. A* **37**, 464 (1988).
- ⁵⁰H. Sekino and R. J. Bartlett, *J. Chem. Phys.* **98**, 3022 (1993).
- ⁵¹M. Stähelin, C. R. Moylan, D. M. Burland, A. Willetts, J. E. Rice, D. P. Shelton, and E. A. Donley, *J. Chem. Phys.* **98**, 5595 (1993).
- ⁵²A. Rizzo, S. Coriani, B. Fernández, and O. Christiansen, *Phys. Chem. Chem. Phys.* **4**, 2884 (2002).
- ⁵³M. Pecul, F. Pawłowski, P. Jørgensen, A. Köhn, and C. Hättig, *J. Chem. Phys.* **124**, 114101 (2006).
- ⁵⁴P. Beaujean and B. Champagne, *J. Chem. Phys.* **145**, 044311 (2016).
- ⁵⁵D. M. Bishop, *Rev. Mod. Phys.* **62**, 343 (1990).

- ⁵⁶D. M. Bishop and B. Kirtman, *J. Chem. Phys.* **95**, 2646 (1991).
- ⁵⁷D. M. Bishop and B. Kirtman, *J. Chem. Phys.* **97**, 5255 (1992).
- ⁵⁸D. M. Bishop, J. M. Luis, and B. Kirtman, *J. Chem. Phys.* **108**, 10013 (1998).
- ⁵⁹P. Norman, Y. Luo, and H. Ågren, *J. Chem. Phys.* **109**, 3580 (1998).
- ⁶⁰O. Quinet and B. Champagne, *J. Chem. Phys.* **109**, 10594 (1998).
- ⁶¹D. M. Bishop, F. L. Gu, and S. M. Cybulski, *J. Chem. Phys.* **109**, 8407 (1998).
- ⁶²Q. Quinet and B. Champagne, in *New Trends in Quantum Systems in Chemistry and Physics*, Vol. 6 (Kluwer Academic Publishers, Dordrecht, 2002) pp. 375–392.
- ⁶³M. Torrent-Sucarrat, J. M. Luis, M. Duran, and M. Solà, *J. Chem. Phys.* **120**, 10914 (2004).
- ⁶⁴M. Torrent-Sucarrat, J. M. Luis, and B. Kirtman, *J. Chem. Phys.* **122**, 204108 (2005).
- ⁶⁵J. M. Luis, H. Reis, M. Papadopoulos, and B. Kirtman, *J. Chem. Phys.* **131**, 034116 (2009).
- ⁶⁶O. Loboda, R. Zalesny, A. Avramopoulos, J.-M. Luis, B. Kirtman, N. Tagmatarchis, H. Reis, and M. G. Papadopoulos, *J. Phys. Chem. A* **113**, 1159 (2009).
- ⁶⁷B. Skwara, R. W. Góra, R. Zalesny, P. Lipkowski, W. Bartkowiak, H. Reis, M. G. Papadopoulos, J. M. Luis, and B. Kirtman, *J. Phys. Chem. A* **115**, 10370 (2011).
- ⁶⁸A. Avramopoulos, H. Reis, J. M. Luis, and M. G. Papadopoulos, *J. Comput. Chem.* **34**, 1446 (2013).
- ⁶⁹B. Orr and J. Ward, *Mol. Phys.* **20**, 513 (1971).
- ⁷⁰B. Kirtman and J. M. Luis, *Int. J. Quant. Chem.* **111**, 839 (2011).
- ⁷¹R. Bersohn, Y.-H. Pao, and H. L. Frisch, *J. Chem. Phys.* **45**, 3184 (1966).
- ⁷²D. L. Andrews and P. Allcock, *Optical Harmonics in Molecular Systems* (Wiley-VCH, Weinheim, 2002) oCLC: ocm48468465.
- ⁷³J. S. Ford and D. L. Andrews, *J. Phys Chem. A* **122**, 563 (2018).
- ⁷⁴P. Beaujean and B. Champagne, *Theor. Chem. Acc.* **137**, 50 (2018).
- ⁷⁵O. Christiansen, H. Koch, and P. Jørgensen, *Chem. Phys. Lett.* **243**, 409 (1995).
- ⁷⁶G. D. Purvis and R. J. Bartlett, *J. Chem. Phys.* **76**, 1910 (1982).
- ⁷⁷T. H. Dunning, *J. Chem. Phys.* **90**, 1007 (1989).
- ⁷⁸K. Hald, A. Halkier, P. Jørgensen, and S. Coriani, *J. Chem. Phys.* **117**, 9983 (2002).
- ⁷⁹C. Hättig, O. Christiansen, H. Koch, and P. Jørgensen, *Chem. Phys. Lett.* **269**, 428 (1997).

- ⁸⁰O. Christiansen, J. Gauss, and J. F. Stanton, *Chem. Phys. Lett.* **305**, 147 (1999).
- ⁸¹C. Hättig, *Chem. Phys. Lett.* **296**, 245 (1998).
- ⁸²C. Hättig and P. Jørgensen, *Adv. Quantum Chem.* **35**, 111 (1999).
- ⁸³L. F. Richardson and J. A. Gaunt, *Philos. Trans. Royal Soc. A* **226**, 299 (1927).
- ⁸⁴J. E. Bloor, *Comput. Theor. Chem.* **234**, 173 (1991).
- ⁸⁵A. A. K. Mohammed, P. A. Limacher, and B. Champagne, *J. Comput. Chem.* **34**, 1497 (2013).
- ⁸⁶M. de Wergifosse, V. Liégeois, and B. Champagne, *Int. J. Quant. Chem.* **114**, 900 (2014).
- ⁸⁷M. E. Wieser, *Pure Appl. Chem.* **78**, 2051 (2006).
- ⁸⁸K. Aidas, C. Angeli, K. L. Bak, V. Bakken, R. Bast, L. Boman, O. Christiansen, R. Cimiraglia, S. Coriani, P. Dahle, E. K. Dalskov, U. Ekström, T. Enevoldsen, J. J. Eriksen, P. Ettenhuber, B. Fernández, L. Ferrighi, H. Fliegl, L. Frediani, K. Hald, A. Halkier, C. Hättig, H. Heiberg, T. Helgaker, A. C. Hennum, H. Hettema, E. Hjertenæs, S. Høst, I.-M. Høyvik, M. F. Iozzi, B. Jansík, H. J. Aa. Jensen, D. Jonsson, P. Jørgensen, J. Kauczor, S. Kirpekar, T. Kjærgaard, W. Klopper, S. Knecht, R. Kobayashi, H. Koch, J. Kongsted, A. Krapp, K. Kristensen, A. Ligabue, O. B. Lutnæs, J. I. Melo, K. V. Mikkelsen, R. H. Myhre, C. Neiss, C. B. Nielsen, P. Norman, J. Olsen, J. M. H. Olsen, A. Osted, M. J. Packer, F. Pawłowski, T. B. Pedersen, P. F. Provasi, S. Reine, Z. Rinkevicius, T. A. Ruden, K. Ruud, V. V. Rybkin, P. Salek, C. C. M. Samson, A. S. de Merás, T. Saue, S. P. A. Sauer, B. Schimmelpfennig, K. Sneskov, A. H. Steindal, K. O. Sylvester-Hvid, P. R. Taylor, A. M. Teale, E. I. Tellgren, D. P. Tew, A. J. Thorvaldsen, L. Thøgersen, O. Vahtras, M. A. Watson, D. J. D. Wilson, M. Ziolkowski, and H. Ågren, *WIREs Comput. Mol. Sci.* **4**, 269 (2014).
- ⁸⁹G. Maroulis, *Chem. Phys. Lett.* **289**, 403 (1998).
- ⁹⁰T. Kobayashi, K. Sasagane, F. Aiga, and K. Yamaguchi, *J. Chem. Phys.* **110**, 11720 (1999).
- ⁹¹T. Kobayashi, K. Sasagane, F. Aiga, and K. Yamaguchi, *J. Chem. Phys.* **111**, 842 (1999).
- ⁹²D. Spelsberg and W. Meyer, *J. Chem. Phys.* **108**, 1532 (1998).
- ⁹³D. Bokhan and R. J. Bartlett, *J. Chem. Phys.* **127**, 174102 (2007).
- ⁹⁴A. J. Russell and M. A. Spackman, *Mol. Phys.* **84**, 1239 (1995).
- ⁹⁵J. M. Luis, M. Duran, J. L. Andrés, B. Champagne, and B. Kirtman, *J. Chem. Phys.* **111**, 875 (1999).

- ⁹⁶O. Quinet, B. Champagne, and B. Kirtman, *J. Comput. Chem.* **22**, 1920 (2001).
- ⁹⁷O. Quinet, B. Kirtman, and B. Champagne, *J. Chem. Phys.* **118**, 505 (2003).
- ⁹⁸A. J. Sadlej, *Collect. Czech. Chem. Commun.* **53**, 1995 (1988).
- ⁹⁹M. J. Cohen, A. Willetts, R. D. Amos, and N. C. Handy, *J. Chem. Phys.* **100**, 4467 (1994).
- ¹⁰⁰J. Kongsted and O. Christiansen, *J. Chem. Phys.* **125**, 124108 (2006).
- ¹⁰¹O. Christiansen, J. Kongsted, M. J. Paterson, and J. M. Luis, *J. Chem. Phys.* **125**, 214309 (2006).
- ¹⁰²M. B. Hansen, O. Christiansen, and C. Hättig, *J. Chem. Phys.* **131**, 154101 (2009).
- ¹⁰³M. B. Hansen and O. Christiansen, *J. Chem. Phys.* **135**, 154107 (2011).
- ¹⁰⁴D. M. Bishop, B. Kirtman, H. A. Kurtz, and J. E. Rice, *J. Chem. Phys.* **98**, 8024 (1993).
- ¹⁰⁵D. M. Bishop and E. K. Dalskov, *J. Chem. Phys.* **104**, 1004 (1996).
- ¹⁰⁶H. Reis, S. Raptis, and M. Papadopoulos, *Chem. Phys.* **263**, 301 (2001).
- ¹⁰⁷A. J. Thorvaldsen, K. Ruud, and M. Jaszuński, *J. Phys. Chem. A* **112**, 11942 (2008).
- ¹⁰⁸G. Katzer, “Character Tables,” http://gernot-katzers-spice-pages.com/character_tables/. Accessed on 11 January 2019.